JOURNAL OF APPLIED ELECTROCHEMISTRY 25 (1995) 501–507

Effect of sulphate anions on tunnel etching of aluminium

J. FLIS

Institute of Physical Chemistry of the Polish Academy of Sciences, 01-224 Warsaw, Poland

L. KOWALCZYK

Tele and Radio Research Institute, 03-450 Warsaw, Poland

Received 9 December 1993; revised 8 November 1994

Electrochemical etching of hard aluminium foil was studied at 100 °C in NaCl solutions without and with Na_2SO_4 in concentrations up to 1.0 M. Addition of Na_2SO_4 resulted in an increase in electric capacitance, in refinement of etch configuration and in an increase in tunnel density per unit volume. A decrease in the number of pits from which the tunnels grew also occurred. The capacitance increased with increasing concentration of Na_2SO_4 up to about 0.35 M, and then decreased. Sulphate ions depressed the formation of pits on the outer oxide-covered surface, but enhanced the growth of the pits and the formation of tunnels from the pits. It is suggested that the retardation of pit nucleation and the acceleration of tunnel growth in the presence of SO_4^{2-} ions can be explained by a partial replacement of Cl^- ions from the oxide and metal surface, respectively. Smaller diameter tunnels may be due to the formation of $Al_2(SO_4)_3$ which can, in part, replace more aggressive $AlCl_3$, and to an easier formation of a passivating film on the tunnel walls owing to their slower dissolution in the presence of $Al_2(SO_4)_3$.

1. Introduction

Electrochemical etching of aluminium foils is widely used in the manufacture of electrolytic capacitor electrodes [1–3]. It results in an enlargement of the surface area and, thus, in an increased capacitance per unit volume. The etching is performed in concentrated chloride solutions at high temperature (up to about 100 °C) with d.c. or a.c. Etching with d.c., at current densities of the magnitude order 1 A cm^{-2}, produces fine tunnels which grow along the ⟨1 0 0⟩ crystallographic direction [2, 4]; these are typically 0.4–2.0 μm wide and 20–50 μm long; their surface density is of the order 10^6–10^8 cm^{-2} [1, 2].

Tunnels grow in the metal which undergoes a crystallographic attack. At ambient temperature they can grow from corrosion pits at potentials slightly above the pitting potential, where crystallographic dissolution occurs [4, 5]; various aspects of pitting have been described by Smialowska [6]. The tunnel growth at high temperature was considered by Alwitt *et al.* [7] as a unique form of pitting corrosion with a sustained balance between dissolution and passivation processes.

Proprietary electrolytic baths for aluminium foil etching contain various additives, among which sodium sulphate is the most common. Sulphate additions considerably increase the capacitance of foils [1, 2, 8–10] owing to the refinement of the etch configuration [1].

Sulphate ions also affect pitting corrosion of aluminium [10–16]. Hampson *et al.* [10] reported that in concentrated NaCl solutions the breakdown potential can be shifted in the noble direction by sulphate ions only at concentrations above 0.3 M. In a solution of 10^{-2} M NaCl of pH 11, Hunkeler and Böhni [16] observed an elongation of the induction time, when sulphate concentration was 0.1 M and higher. An acceleration of the pit growth was ascribed by these authors to the rise in the solution conductivity.

The present work examines the effect of sulphate ions on the initial and later stages of aluminium etching in hot NaCl solutions of varying concentration. A possible explanation of the role of sulphate ions in the tunnel initiation and propagation has been proposed.

2. Experimental details

Measurements were performed on hard-rolled, 85 μm thick aluminium capacitor grade foil (99.99 wt % Al; 30 Fe, 14 Cu and 5 ppm Mg) which is used for the manufacture of electrolytic capacitor anodes. Specimens were cleaned in 3% NaOH for 30 s at ambient temperature, rinsed with deionized water, dried in air and mounted in a holder leaving an exposed surface area of 1.0 cm^2 (for transient measurements the area was 0.07 cm^2). Measurements were performed at temperature of 100 °C in NaCl solutions at concentrations from 1.9 M up to 4.1 M without and with addition of Na_2SO_4 in concentrations up to 1.0 M, of pH 7.1 (pH was measured at 80 °C); some measurements were carried out in a solution with added HCl to adjust the pH to 2.4 (at 80 °C). The solutions were prepared from deionized water

0021-891X

and analytical reagent grade chemicals. Electrode potentials were recorded and are reported relative to a saturated calomel electrode (SCE).

Electrochemical measurements were started from a potential of −1.4 V vs SCE after polarizing the specimen at this potential for 120 s. Voltammograms were measured at a sweep rate of 6.7 mV s^{-1}. Galvanostatic transients were recorded with a storage oscilloscope.

The capacitance of as-etched specimens (without anodic formation of an oxide layer) was measured at a frequency of 50 Hz in 5% H_3BO_3 with NH_3 aq. added to adjust the resistivity to 50 Ω cm at 70 °C.

Outer surface and cross sections were examined with SEM. The cross sections were prepared from foils which were anodically oxidized in 6% H_3BO_3 at 30 V to fill the tunnels with oxides. After electrolytic polishing of the cross sections, the aluminium matrix was dissolved, and the exposed oxides were sputter coated with gold.

3. Results

3.1. *Voltammograms and characteristic potentials*

The potential was swept from −1.4 V vs SCE in the noble direction until the anodic current reached 0.5 A cm^{-2}. The potential was then reversed. Figure 1 shows typical voltammograms for aluminium foil in 2.0 M NaCl of pH 7.1 and 2.4 (adjusted with HCl). Arrows indicate potentials characteristic of pitting corrosion [6]: (a) pitting potential E_p, where stable pits nucleate, (b) repassivation potential E_{rp}, where the existing pits repassivate and stop growing, (c) inhibition potential E_i, where the pit growth is inhibited at potentials nobler than E_p. These potentials are associated with the formation of pits and tunnels.

Upon sweep reversal, the backward curves for pH 7.1 lay at more active potentials than the forward curves ($E_{rp} < E_p$), whereas for pH 2.4 they lay at nobler potentials ($E_i > E_p$). In the latter case the etch pits were distributed more uniformly than in the former one, as reported for NaCl and HCl solutions by Alwitt *et al.* [7].

The slope of the polarization lines at potentials above E_p was about 0.2 Ω cm^2, being close to the solution resistance between Luggin probe and the electrode. This indicates that the slope can be ascribed to the ohmic polarization. The lack of an activation polarization during tunnel or pit growth in aluminium was also reported elsewhere [7, 18].

In solutions of pH 7.1, E_p and E_{rp} decreased with increasing NaCl concentration (Fig. 2) in accordance with the known relationship [6]:

$$E_p = A - B\log[X^-] \qquad (1)$$

where $[X^-]$ is the concentration of the aggressive anion, and A and B are constants.

The slope for E_{rp} (0.16 V) was smaller than that for E_p (0.33 V), demonstrating that the repassivation of pits or tunnels depends less on the bulk solution composition than does their nucleation. The repassivation is determined mainly by the solution composition within the pits and/or tunnels. Solutions in such occluded cells are characterized by higher concentration of chloride anions and of protons than that outside of the occluded cells [6].

The voltammetric measurements did not show any noticeable effect of Na_2SO_4 in concentrations up to 0.3 M on E_p or E_{rp} (Figs 2 and 3).

3.2. *Capacitance*

Figure 4 shows the dependence of the capacitance of aluminium foil on concentration of NaCl in solutions with 0.1 M and 0.3 M Na_2SO_4. The capacitance was measured on as-etched specimens after single sweep cycles from −1.4 V vs SCE to −0.76 V vs SCE and back to −1.4 V vs SCE.

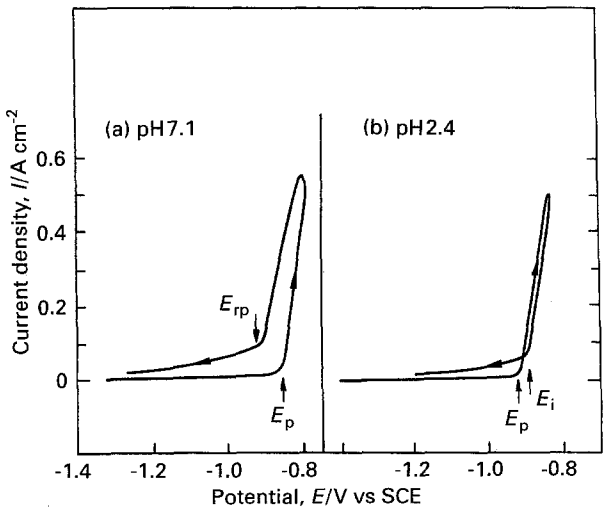

Fig. 1. Voltammograms for Al foils in 2.0 M NaCl at 100 °C of (a) pH 7.1 and (b) 2.4. E_p, E_{rp} and E_i are pitting, repassivation and inhibition potentials, respectively. Sweep rate, 6.7 mV s^{-1}.

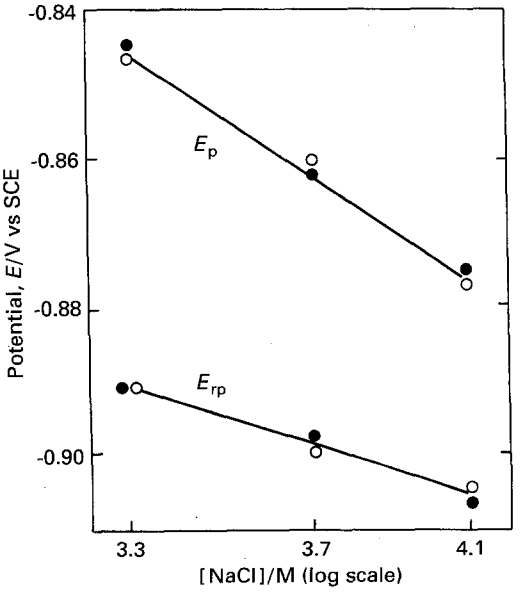

Fig. 2. Effect of NaCl concentration on pitting and repassivation potentials (E_p and E_{rp}) in solutions with Na_2SO_4. Key: (●) 0.1 M Na_2SO_4 and (○) 0.3 M Na_2SO_4 at pH 7.1.

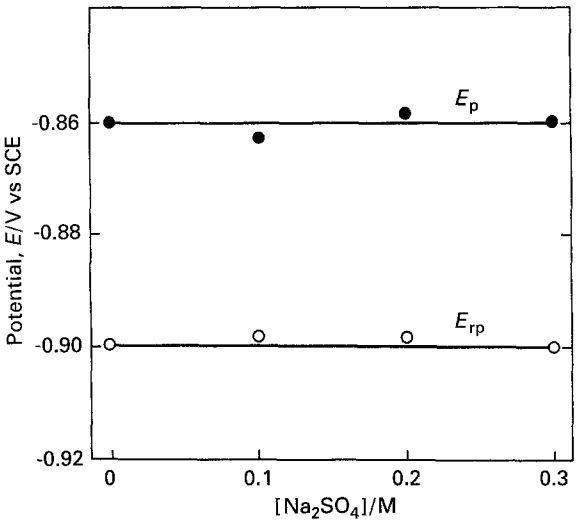

Fig. 3. E_p and E_{rp} as a function of Na_2SO_4 concentration in 3.7 M NaCl at pH 7.1.

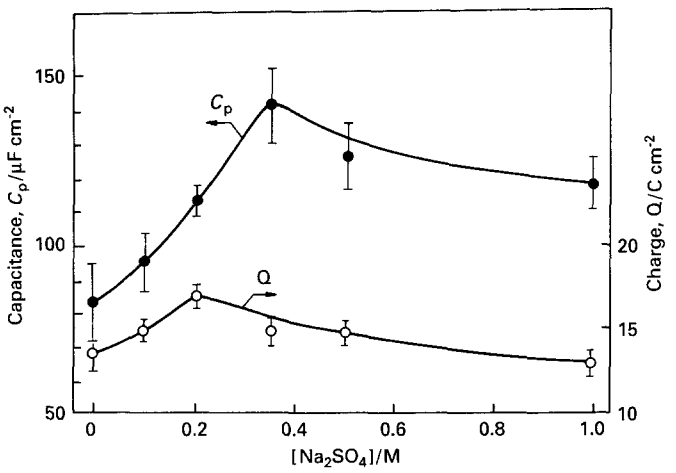

Fig. 5. Effect of Na_2SO_4 concentration on capacitance and anodic charge after polarization in 2.8 M NaCl at −0.76 V vs SCE for 60 s at pH 7.1.

The capacitance rose as the NaCl concentration increased above 2.8 M, evidently due to the shift of E_p in the active direction (Fig. 2) and hence larger difference between E_p and the potential of −0.76 V vs SCE. For the solutions with 0.3 M Na_2SO_4 the capacitance was typically higher than for those with 0.1 M Na_2SO_4, however, this tendency was reversed for NaCl concentrations above 4 M.

Figure 5 shows the dependence of the capacitance, and of the anodic dissolution charge, on the Na_2SO_4 concentration in 2.8 M NaCl after potentiostatic etching for 60 s at −0.76 V vs SCE. At this potential anodic current was within the range of currents used in the manufacture of electrolytic capacitors [1–3]. The capacitance increased as the Na_2SO_4 concentration increased up to 0.35 M Na_2SO_4, and then it decreased slightly. The rise in the anodic dissolution charge was significantly smaller than the rise in the capacitance. This suggests that Na_2SO_4 increased the capacitance by changing the etch configuration, rather than by enhancing the total dissolution.

3.3. *Galvanostatic transients*

Figure 6 presents galvanostatic transients for aluminium foil in 3.7 M NaCl without and with 0.3 M Na_2SO_4, acidified to pH 2.4. The initial rise in potential is associated with double layer charging and oxide growth, whereas its decrease, after the attainment of the maximum, can be ascribed to a breakdown of the oxide film, and to subsequent nucleation of pits and tunnels. Potential and time at the maximum are denoted as the pit nucleation potential, E_{pn}, and breakdown time, T_b, respectively. The subsequent stabilization of the potential at a lower level indicates the attainment of a steady growth of either pits or tunnels (pit growth potential, E_{pg}).

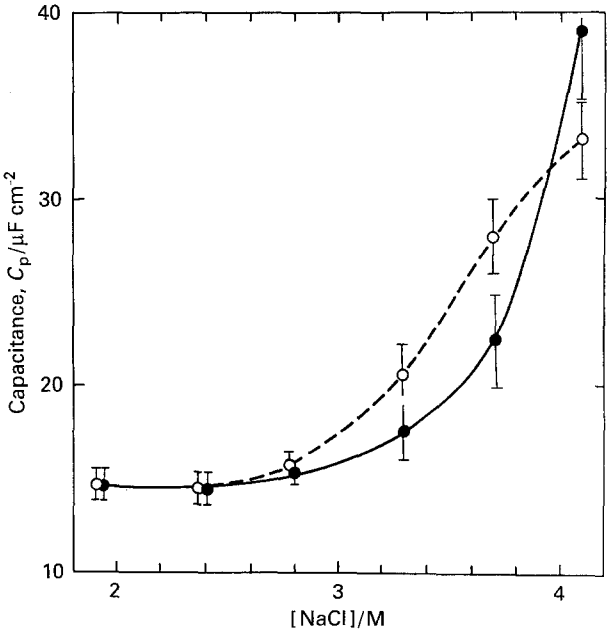

Fig. 4. Effect of NaCl concentration on capacitance after a voltammetric cycle from −1.4 V vs SCE to −0.76 V vs SCE and reverse at scan rate of 6.7 mV s^{-1} in solutions with (●) 0.1 M Na_2SO_4 and (○) 0.3 M Na_2SO_4 at pH 7.1.

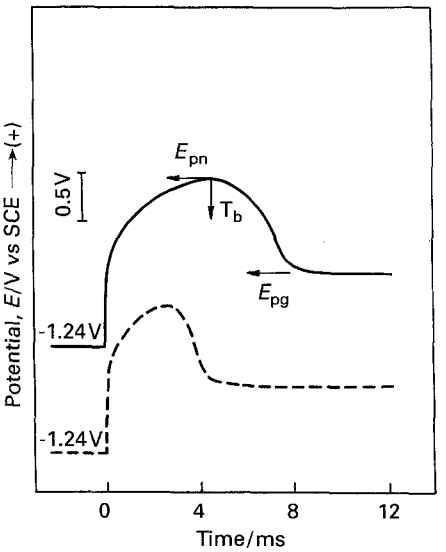

Fig. 6. Galvanostatic transients in 3.7 M NaCl acidified to pH 2.4, (– – –) without and (——) with 0.3 M Na_2SO_4. E_{pn} is potential of pit nucleation, T_b is breakdown time, and E_{pg} is potential of pit growth. Current density: 2.0 A cm^{-2}.

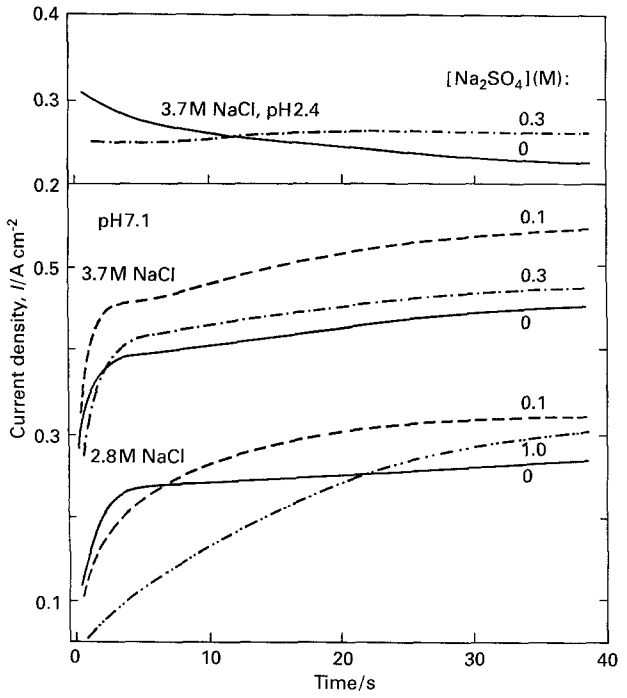

Fig. 7. Current against time of polarization at −0.76 V vs SCE in NaCl solutions of pH 7.1 and 2.4, without and with Na_2SO_4.

The breakdown time, T_b, and time to the attainment of E_{pg} were longer in the Na_2SO_4-containing solution than in the Na_2SO_4-free solution. The extension of T_b indicates that Na_2SO_4 makes the film breakdown more difficult.

3.4. *Current against time at a constant potential*

During the polarization of aluminium foils at −0.76 V vs SCE, the anodic current decreased with time in the acidic NaCl solution (pH 2.4), whereas it increased with time in the neutral solutions (pH 7.1) (Fig. 7). The rise in the current with time was also reported by Fickelscher [17]. An addition of Na_2SO_4 resulted in a decrease in the current in the early stages of polarization, and an increase in the later stages (Fig. 7).

Figure 8 shows current against Na_2SO_4 concentration in the early stage of polarization (at 2 s) and

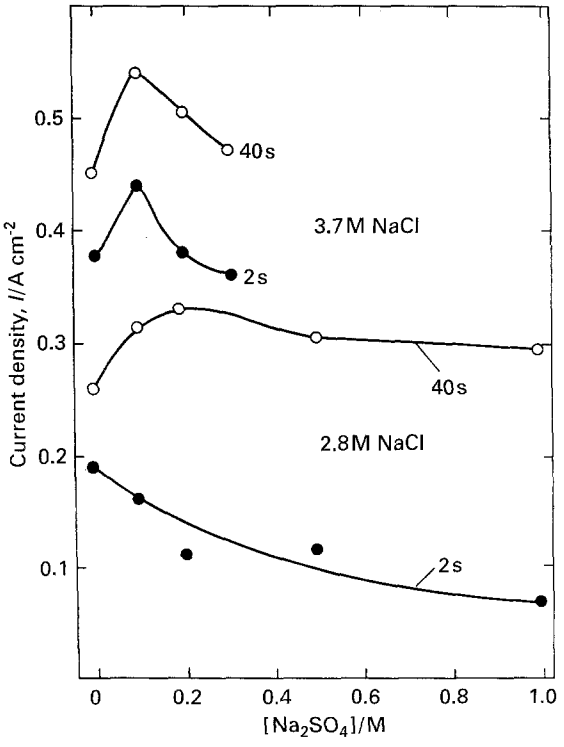

Fig. 8. Current during polarization at −0.76 V vs SCE at 2 s and 40 s as a function of Na_2SO_4 concentration at pH 7.1.

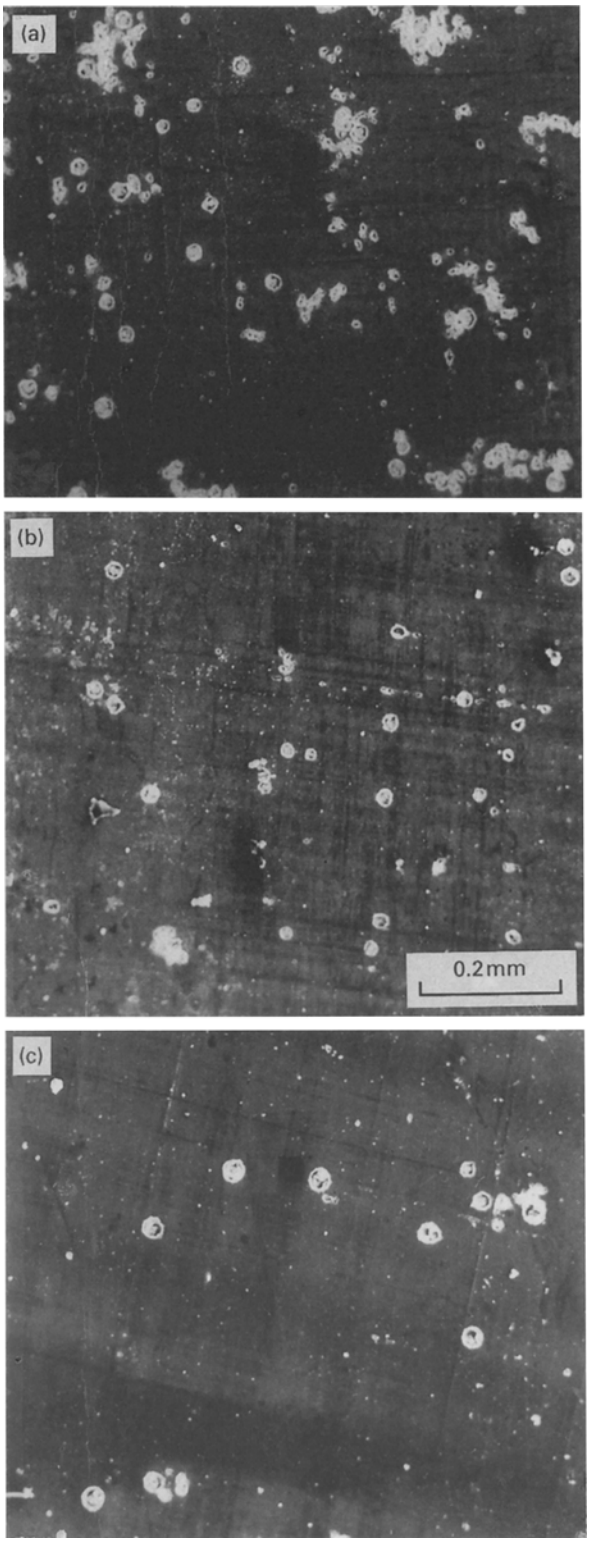

Fig. 9. Surface of Al foil after etching at −0.76 V vs SCE for 60 s in 3.7 M NaCl, pH 7.1; (a) without additions, (b) with 0.1 M Na_2SO_4, (c) with 0.3 M Na_2SO_4. Capacitance for (a), (b) and (c) was 180, 230 and 280 μF cm^{-2}, respectively.

in the later stage (40 s). In the early stage the current in 2.8 M NaCl decreased with the increasing Na_2SO_4 concentration, whereas in the more concentrated solution of 3.7 M NaCl it exhibited a maximum. In the later stage the current showed a maximum in both solutions.

The decrease in the initial current suggests that Na_2SO_4 improves the resistance of an oxide film against attack by chloride ions. The maxima indicate that, depending on the concentration and polarization stage, Na_2SO_4 can accelerate or retard anodic processes on aluminium. The former effect prevails at low concentrations of Na_2SO_4, whereas the latter effect appears at high concentrations.

3.5. *Morphology of etching*

SEM micrographs of the outer surface (Fig. 9) show that the addition of Na_2SO_4 resulted in the formation of larger pits, but at smaller surface density than in the Na_2SO_4-free solution; simultaneously, the capacitance increased. This shows that in the presence of Na_2SO_4 the pit nucleation becomes more difficult, hence, the surface film is more resistant to chloride attack.

The same effect of Na_2SO_4 is seen on the cross sections of etched foils (Fig. 10). The micrographs show that in the presence of Na_2SO_4 the pits are less in number, but larger and with a greater number of tunnels. The tunnels grew only inside the pits, but never from the outer surface.

At the higher magnification it can be seen (Fig. 11) that, in the presence of Na_2SO_4, the etch structure is finer, with tunnels being narrower and more numerous.

This morphology suggests that the initially lower current in the presence of SO_4^{2-} ions (Figs 7 and 8) is associated with a smaller number of pits (more difficult pit nucleation), whereas the higher current in the later stages is associated with a faster growth of pits and tunnels.

4. Discussion

Additions of Na_2SO_4 resulted in an extension of the breakdown time T_b (Fig. 6) and in a decrease in the number of corrosion pits (Figs 9 and 10), suggesting a rise in the resistance of the aluminium oxide film to breakdown. This may be due to a partial replacement from the oxide film of Cl^- by less aggressive SO_4^{2-}, as a result of competitive adsorption of these two anions. Rozenfeld and Maksimchuk [19] showed by radioactive measurements that adsorption of Cl^- on chromium powder was decreased in the presence of SO_4^{2-}, whereas Maitra [20] reported, on the basis of an AES investigation, that incorporation of Cl^- in the passive film on aluminium decreased with increasing concentration of SO_4^{2-} in Cl^-/SO_4^{2-} solutions.

As well as making the oxide film more resistant to the chloride attack, sulphate anions increase the anodic dissolution after film breakdown, as manifested by the rising current in the later stages of the polarization (Fig. 7) and by the larger size of the pits (Fig. 10). Pits dissolve actively, and a salt film is likely to form at their surface [21, 22]. Active dissolution of metals can be inhibited by chloride and other halide anions due to replacement of OH^- ions, which participate in the anodic reaction [23, 24]. Probably, a partial replacement of inhibiting Cl^- by SO_4^{2-} can be a reason for the faster dissolution in the pits.

Sotoudeh *et al.* [25] have found that the corrosion rate of aluminium alloys at ambient temperature in acidic solutions of pH between 2.6 and 3.5 is faster

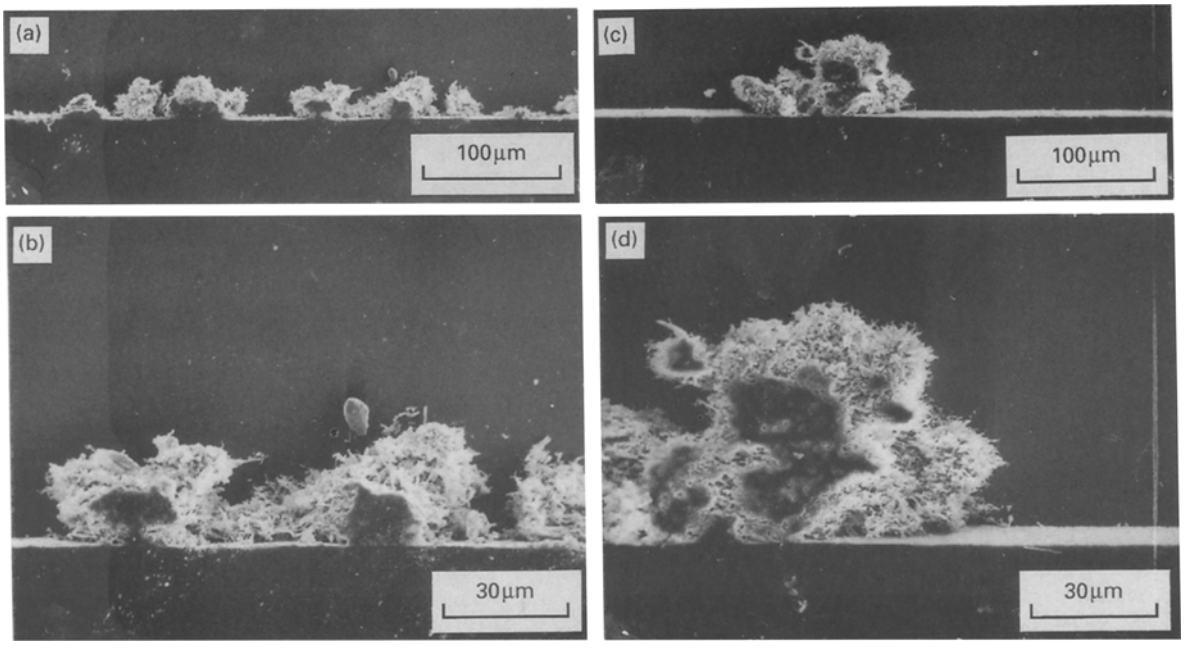

Fig. 10. Cross section of Al foil etched at −0.76 V vs SCE for 60 s in 2.8 M NaCl without Na_2SO_4 ((a) and (b)) and with 0.35 M Na_2SO_4 ((c) and (d)).

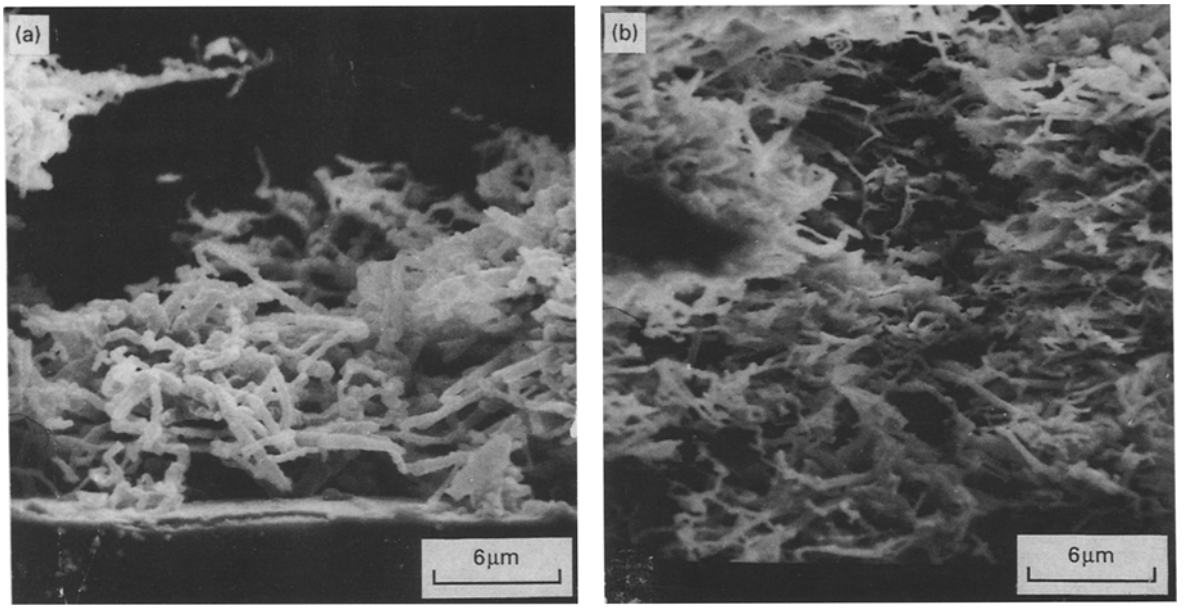

Fig. 11. Cross section of Al foil etched as in Fig. 10; (a) without Na_2SO_4, (b) with 0.35 M Na_2SO_4.

in $Al_2(SO_4)_3$ solutions than in NaCl solutions, but slower than in $AlCl_3$ solutions. $Al_2(SO_4)_3$ is formed during anodic dissolution of aluminium in SO_4^{2-}-containing solutions; hence, it can be supposed that sulphate anions may accelerate corrosion of aluminium in NaCl solutions, but slow it down in $AlCl_3$ solutions. The former situation may occur at sites where the bulk NaCl solution has easy access to the dissolving metal (nuclei of pits or tunnels), whereas the latter situation can occur in occluded cells, where high concentration of $AlCl_3$ builds up (inside tunnels).

Tunnel etching involves processes occurring on the outer oxide-covered surface, inside the pits, and inside the tunnels, at their tips and walls. In this work it is suggested that the effect of sulphate anions on the related processes can be as depicted in Fig. 12 and described below.

4.1. *Nucleation of pits on the outer surface*

Pits can be nucleated by any of the mechanisms proposed for pit initiation [6], involving local agglomeration of aggressive Cl^- anions. Sulphate anions counteract this agglomeration by a competitive adsorption on the oxide surface. As a result, the pits

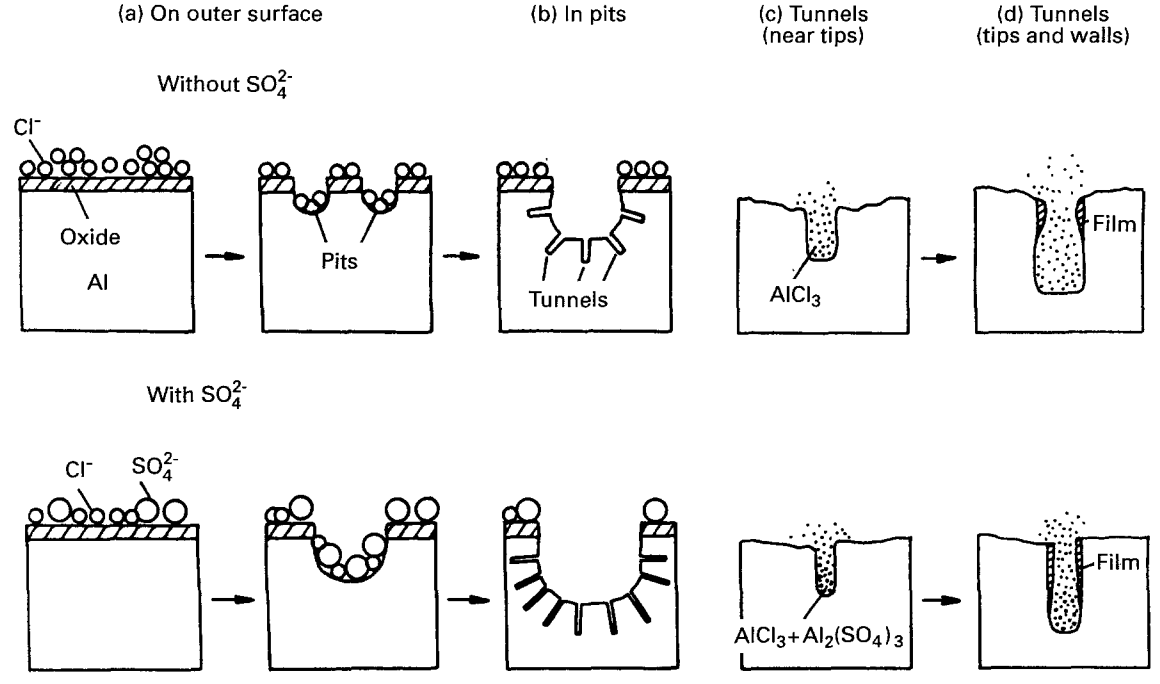

Fig. 12. Schematic presentation of etch stages on Al foil and of the suggested effect of sulphate anions. (a) Initiation of pits is retarded by SO_4^{2-} ions owing to the competitive adsorption with Cl^- ions on the oxide surface. (b) Initiation of tunnels in pits is facilitated by SO_4^{2-} ions owing to replacement from the metal surface of Cl^- ions which inhibit active dissolution. (c) Dissolution of tunnel walls at the tips can be slower due to the formation of $Al_2(SO_4)_3$ which partially replaces more aggressive $AlCl_3$. (d) Passivating film on the tunnel walls can form easier owing to the slower dissolution in the presence of $Al_2(SO_4)_3$.

form after a longer induction time and on a smaller number of sites.

4.2. *Nucleation of tunnels in pits*

Sulphate anions adsorb competitively, not only on the outer oxide surface, but also on the metal surface inside the pits. Chloride anions inhibit active dissolution of metals, hence their replacement by SO_4^{2-} anions may facilitate the pit growth and tunnel initiation. As a result, the size of pits and number of tunnels are larger.

4.3. *Dissolution at the tunnel tips*

All the anions diffuse towards the tunnel tip. Therefore, in the presence of SO_4^{2-}, $Al_2(SO_4)_3$ forms in addition to $AlCl_3$. $Al_2(SO_4)_3$ is less aggressive than $AlCl_3$; hence the dissolution of tunnel walls is slower. As a result, the tunnel tips are narrower.

4.4. *Passivation of tunnel walls*

As a consequence of the slower dissolution in the presence of $Al_2(SO_4)_3$, the formation of a passivating film on tunnel walls will be easier. Additionally, in the presence of sulphate anions the film may be more protective owing to partial replacement of Cl^- by SO_4^{2-}. As a result, the tunnels are narrower.

This explanation appears to be consistent with the present results and published data.

5. Conclusions

(i) Electrochemical etching of aluminium foil in hot NaCl solutions is promoted by Na_2SO_4. Addition of Na_2SO_4 to NaCl solutions resulted in the formation of pits less in number but larger in size, and in more intense growth of tunnels from the pits. The tunnels were narrower and more numerous. The capacitance of foils etched in the presence of Na_2SO_4 was enhanced.

(ii) It is proposed that the effect of sulphate anions on the etching can be explained as follows: (a) nucleation of pits on the outer oxide-covered surface is retarded by SO_4^{2-} anions owing to their competitive adsorption with Cl^- anions, which strongly deteriorate the oxide film; (b) nucleation of tunnels in pits is facilitated owing to the competitive adsorption on the metal surface, resulting in replacement of Cl^- anions which inhibit active dissolution of metals; (c) tunnels are narrower because $Al_2(SO_4)_3$ can form in addition to $AlCl_3$, the former being less aggressive to aluminium than the latter. As a result, the dissolution of tunnel walls is slower and, therefore, the formation of the passivating film is facilitated.

References

[1] M. S. Hunter, *J. Electrochem. Soc.* **117** (1970) 1215.
[2] C. G. Dunn, R. B. Bolon, A. S. Alwan and A. W. Stirling, *ibid.* **118** (1971) 381.
[3] N. F. Jackson, *Electrocomp. Sci. Techn.* **2** (1975) 33.
[4] C. Edeleanu, *J. Inst. Metals* **89** (1960) 90.
[5] J. A. Richardson and G. C. Wood, *Corros. Sci.* **10** (1970) 313.
[6] Z. Szklarska-Smialowska, 'Pitting Corrosion of Metals', NACE, Houston (1986).
[7] R. S. Alwitt, H. Uchi, T. R. Beck and R. C. Alkire, *J. Electrochem. Soc.* **131** (1984) 13.
[8] C. E. Welch, Jr., *US Patent 3 316 164* (1967).
[9] M. T. Kosmynina and K. P. Bartashov, *Zhur. Prikl. Khimii* **6** (1975) 1476.
[10] N. A. Hampson, N. Jackson and B. N. Stirrup, *Surf. Technol.* **5** (1977) 277.
[11] H. Böhni and H. H. Uhlig, *J. Electrochem. Soc.* **116** (1969) 906.
[12] C. Jangg, H. Meissner and R. Zûrner, *Aluminium* **50** (1974) 205.
[13] W. J. Rudd and J. C. Scully, *Corros. Sci.* **20** (1980) 611.
[14] R. R. Wiggle, V. Hospadaruk and E. A. Styloglou, *Mat. Perform.* **20** (1981) 13.
[15] G. Sussek, M. Kesten, H.-G. Feller, *Metall* **33** (1979) 1031, 1276.
[16] F. Hunkeler and H. Böhni, *Werk. Korros.* **34** (1983) 68.
[17] H. Fickelscher, *Werk. Korros.* **33** (1982) 146.
[18] H. Kaesche, *in* 'Localized Corrosion, NACE-3' (edited by R. Staehle, B. Brown, J. Kruger and A. Agrawal), NACE, Houston (1974) p. 516.
[19] I. L. Rozenfeld and V. P. Maksimchuk, *Dokl. Akad. Nauk SSSR* **131** (1960) 354.
[20] S. Maitra, PhD. thesis, University of Florida (1974) (quoted in [6], p. 299).
[21] S. M. De Micheli, *Corros. Sci.* **18** (1978) 605.
[22] T. R. Beck and R. C. Alkire, *J. Electrochem. Soc.* **126** (1979) 1662.
[23] K. Schwabe and C. Voigt, *Electrochim. Acta* **14** (1969) 853.
[24] S. M. Reshetnikov, *Zhur. Prikl. Khimii* **53** (1980) 572.
[25] K. Sotoudeh, T. H. Nguyen, R. T. Foley and B. F. Brown, *Corrosion* **37** (1981) 358.